

Investigation of an Extremely Flexible Stowable Rotor

Jayant Sirohi
Assistant Professor,
Department of Aerospace Engineering and
Engineering Mechanics,
University of Texas at Austin,
Austin, TX 78712

Anubhav Datta
Rotorcraft Dynamicist,
ELORET Corporation,
U. S. Army AFDD,
NASA Ames Research Center,
Moffett Field, CA 94035

Abstract

This paper describes the analysis, fabrication and hover testing of a rotor with extremely flexible carbon-fiber composite rotor blades. The flexibility of the rotor blades is such that they can be rolled into a compact volume and stowed in the rotor hub. While the benefits of a variable-diameter, stowable rotor for full-scale, high-speed helicopters is well known, the present study focuses on application to a micro-helicopter. An 18 inch diameter rotor having untwisted, constant chord blades with a circular arc airfoil profile, is discussed. A comprehensive rotor aeromechanics code is used to analyze the behavior of the flexible rotor blades and to investigate the effect of a tip mass on the rotor stability. The hover performance of a two-bladed rotor with flexible blades is compared to that of a rotor with rigid blades having an identical planform and airfoil section. Stable operation of the flexible rotor in hover was achieved by positioning the tip mass at a suitable chordwise location. A maximum Figure of Merit of 44% was measured for the rigid rotor blades and 22% was measured for the flexible rotor blades. In general, the high twist induced in the flexible rotor blades resulted in a lower thrust and decreased efficiency compared to the rigid rotor blades. Future plans for increasing the efficiency for the flexible rotor blades and expanding the test envelope into forward flight are described.

INTRODUCTION

Helicopters are very efficient at hover and low speed forward flight. This unique ability is accompanied by a maximum speed limited to around 180 knots, which is relatively slow compared to fixed wing aircraft. For several decades, designers have explored aircraft configurations that are capable of high cruise speed, while retaining the favorable low speed attributes of helicopters. The major technical challenges to increasing the maximum speed of a helicopter arise from high Mach numbers encountered by the advancing blade tips, as well as stall occurring on the retreating blades. These two factors combine to decrease the propulsive efficiency of the helicopter rotor at high speeds.

Several approaches have been proposed to overcome these issues. Fradenburgh¹ comprehensively discussed the issues related to high

speed rotary wing aircraft and described some approaches to increasing their maximum speed. Ludi² and Linden³ described the development of several high speed rotary wing aircraft configurations. These approaches typically involve thrust compounding and/or lift compounding. An alternate approach is to incorporate a rigid coaxial system such as in the case of the Sikorsky Advancing Blade Concept (ABC)^{4,5} and the Sikorsky X2 Technology Demonstrator aircraft.^{6,7} The advancing blade tip Mach number can be lowered by decreasing the rotational speed of the rotor in cruise. However, this approach poses several challenges, such as the design of an appropriate drive system, and designing the airframe for a range of excitation frequencies.

For a helicopter to achieve higher speeds than possible with lift and thrust compounding, it becomes necessary to modify the geometry of the rotor. Some helicopters have been designed to completely stop their rotor in cruise. In this case, the rotor must be stable and stiff enough to sustain the aerodynamic loads without excessive

Presented at the AHS 65th Annual Forum, Grapevine, TX, 27-29 May 2009. Copyright © 2009 by AHS International, Inc. All rights reserved.

deflections. All the lift is typically produced by the stopped rotor acting as a wing, as in the case of the Sikorsky X-Wing³ and Boeing Canard Rotor Wing unmanned air vehicle.⁸ Changing the diameter of the rotor blades in flight has also been considered to alleviate some of the aerodynamic issues at high speed. A variable-diameter rotor can be extended to yield a low disk loading that is favorable for hover, and can be retracted in cruise. One such example is the variable-diameter rotor for the Sikorsky Telescoping Rotor AirCRAFT (TRAC).¹ The rotor blades were designed to change their length in flight by means of a differential gear arrangement in the rotor hub that was coupled to the main rotor shaft rotation. Laboratory and wind-tunnel tests were successfully performed on a 9 ft diameter model scale rotor. Airspeeds of up to 400 knots were attained with the rotor in the minimum diameter configuration. The major advantage of the variable-diameter rotor is that the rotational speed remains constant, while the major disadvantage is the additional mechanical complexity and weight added to the rotor system.

In all the above cases, the presence of the rotor blades and rotor hub is still a source of significant drag, which limits the practically achievable maximum cruise speed. Therefore, to achieve even higher speeds several configurations proposed stowing the rotor blades and hub within the fuselage in flight.^{2,3} While conceptually attractive, numerous practical difficulties exist in stopping a rotor in flight, folding the blades and stowing it in the fuselage. Some other configurations proposed a combination of variable-diameter rotor and a stowed rotor. Decreasing the diameter of the rotor before stopping it would result in shorter, stiffer blades with lower aerodynamic forces, and consequently, lower deflections. In addition, the volume required in the fuselage for stowage would be lower, resulting in a smaller fairing and lower drag.

It can be seen that a lightweight, mechanically simple, variable-diameter, stowable rotor is highly attractive for enabling helicopters with a high cruise speed. One design for a stowable rotor consists of a rotor blade that is extremely flexible, so that it can be rolled up into a cylindrical shape and retracted into the rotor hub. Such a design is lighter and simpler compared to the other designs described above. This concept has been explored in several patents⁹⁻¹¹ and studies in the past. Previous studies have typically

involved a rotor blade consisting of some type of thin sheet passively stabilized by centrifugal forces acting on a tip mass. Flexible structural members such as cables or rods are incorporated in the spanwise direction to react the centrifugal loads. This type of rotor blade has essentially no structural stiffness in the bending, torsion or chordwise degrees of freedom, and relies on solely on centrifugal forces for stability.

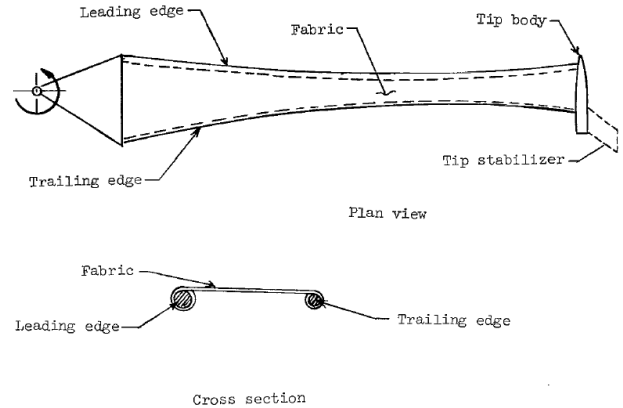
In reality, a flexible rotor blade as described above may not be feasible for full-scale helicopters due to the requirements of high performance airfoils and internal blade structure, as well as the additional hub complexity. However, a flexible rotor is well suited for a micro-helicopter. It has a significant potential in meeting the key objectives of: safety, compact storage, flight stability, durability, and cheap manufacturing. Rotor blades for micro-helicopters typically use a simple circular arc airfoil section.^{12,13} Due to their small size, the structural loads and fatigue requirements for micro-helicopters are not as stringent as for full-scale helicopters. A variable-diameter or stowable rotor also has several advantages for micro-helicopters. For example, the sensitivity of micro-helicopters to gust limits their outdoor flight capability. Reducing the rotor diameter during outdoor cruise flight can decrease the sensitivity of a micro-helicopter to gusts by increasing its disk loading. Indoor flight of micro-helicopters involves a high risk of collision with obstacles. Flexible rotor blades will not be destroyed on impact with obstacles and can result in increased survivability for micro-helicopters performing indoor missions. Clearly, a highly flexible rotor blade is ideally suited for micro-helicopters and has the potential to significantly enhance their flight envelope and survivability. Accordingly, the present study investigates the design and performance of extremely flexible rotor blades of 18 inches diameter, focused on a micro-helicopter application.

STATE OF THE ART

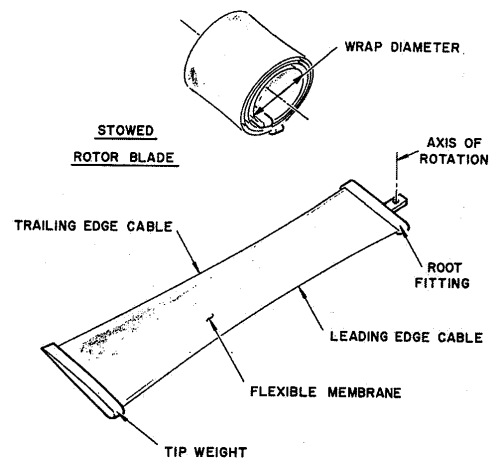
In the late 1960's, Winston¹⁴ investigated flexible rotors for their potential benefits in terms of lower weight and compact storage for large helicopters and convertible aircraft. The rotor blade in this study consisted of a thin non-porous fabric sheet attached to two steel rods that formed the leading and trailing edges of the blade, as shown in Figure. 1(a). A tip mass with an aerodynamic stabilizer was attached to the end of the rotor

blade. The rotor blade was passively stabilized by the centrifugal and aerodynamic forces acting on the tip mass. Analysis of this blade revealed that a careful design of planform as well as tip mass was necessary to ensure aeroelastic stability of the blade as well as stability of the fabric sheet. Experiments were performed on a 30 ft diameter rotor in hover and the performance was compared to a conventional rotor. The Figure of Merit of the flexible rotor was poor, which was attributed to blade deformation. The poor Figure of Merit is not surprising considering that the structural rods resulted in an airfoil section with blunt leading and trailing edges. The flexible rotor achieved higher mean lift coefficients than the conventional rotor due to large camber introduced by aerodynamic forces acting on the fabric. Due to the large tip mass required to ensure stability, the expected weight benefit of the flexible rotor over a conventional rotor could not be substantiated. Because the tip mass also provides chordwise stability, introduction of chordwise stiffeners in the rotor blade resulted in an improved design and a decrease in the required tip mass. A key result of the analysis was that the aeroelastic stability of the flexible rotor blade was independent of the rotational speed. In another study, Winston¹⁵ experimentally investigated the effect of varying the tip mass, aerodynamic stabilizer incidence and tip speed on the hovering performance of a 30 ft diameter flexible rotor. Tip speed was found to be a very important parameter as it affects the camber not only by centrifugal stiffening, but also due to aerodynamic forces. It was concluded that the efficiency of the rotor could be improved by controlling the pitch and stabilizer incidence in addition to designing an appropriate planform. The highest Figures of Merit were measured at low tip speeds, which were considered too low for practical operation.

Pruyn and Swales¹⁶ described the development and testing of a flexible rotor blade at Kellett Aircraft Corporation in the early 1960's. The blade consisted of a fabric or stainless steel membrane between two cables that formed the leading and trailing edges (Figure. 1(b)). A tip mass provided the centrifugal stiffening and the blade could be rolled up into a cylinder. It was shown analytically that the flexible blade weighed only 62.5% of a conventional blade for the same coning angle. In addition, the dynamic stability of the blades was analyzed and was found to be independent of the rotational speed. A ducted two-bladed flexible rotor of diameter 2.9 ft and



(a) NASA rotor blade, from Reference^{14,15}



(b) Kellett rotor blade, from Reference¹⁶

Figure 1. Flexible Rotor Blade Designs

an unducted two-bladed flexible rotor of diameter 4 ft were tested in hover and in axial autorotation in a wind tunnel. The flexible rotors were able to sustain a disk loading of up to 100 psf, however, whirl test data showed poor rotor performance, which was attributed to the high drag of the tip weight as well as leading and trailing edge cables. The study concluded that flexible rotors of this design were feasible and that more analysis was required to establish the stability limits of the rotor. Sikorsky Aircraft Corporation studied an extremely flexible rotor blade that consisted of a thin metal ribbon with a tip mass.¹⁷ This rotor blade could be rolled up into a cylinder and enclosed within the rotor hub. Although promising, the concept was not pursued beyond the model stage in favor of other, lower risk approaches to achieving high speed.

Goldman¹⁸ described the development and hover testing of an extremely flexible rotor at the

Martin Company. The rotor blades consisted of segmented balsa ribs with a flexible skin, supported by 1/16 inch diameter cables at the leading edge and trailing edge. The cables were attached to a tip pod with an electrically driven propeller that provided the torque required by the rotor. In the cases where flutter occurred, a torsional deflection similar to the first mode of a fixed-fixed shaft was observed in high-speed videos. An analysis of the blade including torsion and flapping degrees of freedom was performed using an influence coefficient approach. For a stable blade, it was determined that the blade center of gravity must be ahead of the elastic axis, and the elastic axis must be ahead of the aerodynamic center. It was concluded that it is feasible to design highly flexible, low-disk loading rotors offering significant performance benefits.

Roeseler¹⁹ described the analysis and hover testing of a 3 ft radius, two-bladed ribbon rotor. The blade consisted of a 0.005 inch thick mylar sheet with a tip mass. Theoretical stability boundaries were calculated assuming rigid flapping and linear twisting modes. A position of the tip mass was determined to ensure stability and prevent luffing of the trailing edge. The mylar blade was found to be susceptible to fatigue failure. Stable operation could not be achieved without enclosing the tip mass in an aerodynamic fairing. The same criteria for stability as those discussed by Goldman¹⁸ were determined from the analysis.

PRESENT APPROACH

From the studies described above, it can be seen that the concept of an extremely flexible rotor that can be rolled up into a compact volume appears feasible, both experimentally and analytically. Efficiency of such rotor blades was found to be poor because of low chordwise stiffness of the blades, poor airfoil performance and high drag tip mass. The limits of stability in hover and forward flight have not been fully explored, and no further studies have been reported in the literature on this type of rotor beyond the late 1960's. While the concept appears promising, limited data exists on their behavior, especially at the micro-helicopter scale. It is possible that the performance of these rotors can be enhanced as a result of technological advancements in materials as well as careful design. Key technical challenges as well as possible solutions need to be identified,

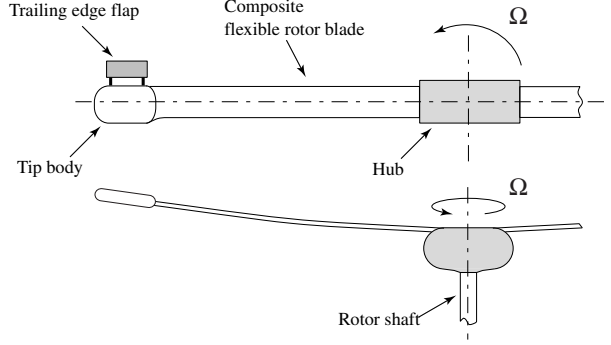
and the present paper documents the beginning of this process.

The flexible rotor blade design explored in the present paper consists of a thin carbon-fiber composite sheet in conjunction with a tip body equipped with an active trailing-edge flap. The design of the flexible rotor blade is focused towards a micro-helicopter applications, and the tip mass is of the same order as the blade mass in order to minimize the total weight of the system. A two-bladed flexible rotor system is shown in the deployed and retracted states in Figure. 2(a) and Figure. 2(b). The composite sheet is designed to sustain the centrifugal loads on the blade, eliminating the need for cables at the leading and trailing edges. The blade cross-section is a circular arc, which results in a more efficient airfoil section than in the previous designs, while retaining sufficient chordwise stiffness. Note that a circular arc airfoil section is very efficient at the low Reynold's numbers at which micro-helicopters operate.^{12,13,20} The trailing-edge flap can provide primary control inputs to the rotor system in addition to performing active stabilization by tip twist control. The active twist control is expected to decrease the total tip mass required for blade stability. The tip body contains a miniature inertial measurement unit (IMU) with which the position of the blade tip can be measured at any instant of time. This IMU provides the sensory feedback for the stabilization and control of the flexible rotor system.

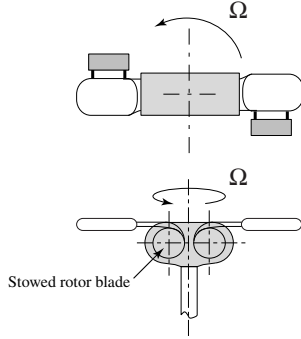
The present paper focuses on the analysis and testing of the flexible composite rotor blade stabilized by a tip mass, and does not address the trailing-edge flap. The hover performance of a 18 inch diameter, two-bladed rotor with flexible blades is measured and compared to that of a rotor with rigid blades having the same planform and airfoil section. The results of these tests will be used to expand the flight envelope of the rotor system into forward flight in future experimental and analytical studies.

PHYSICAL PRINCIPLES

The behavior of a rotor blade with extremely low structural stiffness is dominated by centrifugal forces. For example, in a purely articulated rotor, which has zero stiffness in rigid flap, centrifugal forces result in a fundamental flap frequency of slightly greater than 1/rev. In a similar way, for a rotor blade with negligible torsional stiffness, the



(a) Extended position



(b) Retracted position

Figure 2. Schematic of proposed flexible rotor blade operation

fundamental torsional frequency is slightly greater than 1/rev. Centrifugal forces stiffen the blade in the torsional degree of freedom in two ways - the dumbbell effect and the bifilar effect. The dumbbell effect is also known as the propeller moment, and arises due to the tendency of the centrifugal forces to rotate the rotor blade to flat pitch. The bifilar moment, also known as the trapeze moment, arises from the twisting of the fibers causing an effective shortening of the rotor blade. In conventional rotor blades, the propeller moment is more important. However, in the present case, the bifilar moment can be significant due to the large twist produced in the rotor blade. As an example, consider the case of a flexible rotor blade of constant chord, consisting of a tip mass supported by two cables, forming the leading and trailing edges of the blade. The plan view of the tip such a blade is shown in Figure. 3.

Solving for the tensile forces in each of the cables, we get

$$F_1 = (1 - l/c)m_T\Omega^2 R \quad (1)$$

$$F_2 = l/c m_T\Omega^2 R \quad (2)$$

where l is the position of the center of gravity

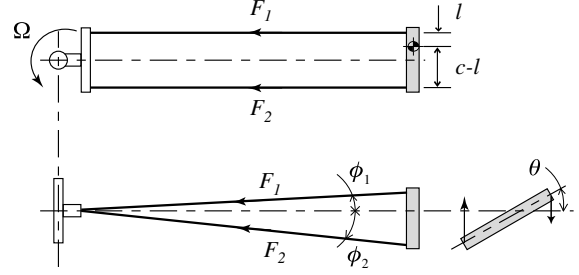


Figure 3. Schematic of bifilar moment in a flexible rotor composed of two cables

of the tip mass, c is the blade chord, m_T is the tip mass, R is the blade radius and Ω is the rotational speed. It can be deduced from the above derivation that the effective elastic axis of the blade is defined by the center of gravity of the tip mass. In the general case, it can be shown that the elastic axis of the rotor blade is defined by the chordwise position of the centroid of the radial stress field along the blade span.^{18,19} Accordingly, for small torsional deflections, the torsional moment on the rotor blade due to the bifilar effect is given by (Figure. 3)

$$M_\theta = F_1 \sin \phi_1 l \theta + F_2 \sin \phi_2 (c - l) \theta \quad (3)$$

where ϕ_1 and ϕ_2 are the angles between the tangent to the cables at the point of attachment to the tip mass and the horizontal plane. Assuming a linear torsional deflection mode shape, the deflected cables will be straight lines, and the relevant angles are given by

$$\sin \phi_1 = l/R \quad (4)$$

$$\sin \phi_2 = (c - l)/R \quad (5)$$

Expressing the bifilar restoring moment in terms of an equivalent torsional stiffness, and substituting for the angles from above,

$$M_\theta = K_\theta \theta \quad (6)$$

$$= l(c - l)m_T\Omega^2 \quad (7)$$

From the above equation, the torsional stiffness due to the bifilar effect is obtained as

$$K_\theta = l(c - l)m_T\Omega^2 \quad (8)$$

and the rotating natural frequency corresponding to the linear deflection mode is

$$\frac{\omega_\theta}{\Omega} = \sqrt{\frac{m_T c^2}{I_T} \left(\frac{l}{c} - \frac{l^2}{c^2} \right)} \quad (9)$$

where I_T is the torsional moment of inertia of the tip mass about its center of gravity. The variation of torsional frequency with chordwise position of the tip mass center of gravity is plotted in Reference. 16. Note that for a cylindrical tip mass of uniform density ($I_T = m_T c^2/12$), the maximum torsional frequency occurs when the tip mass is centered between the two cables ($l/c = 0.5$). In this condition, the torsional frequency becomes $\omega_\theta/\Omega = \sqrt{3} = 1.732/\text{rev}$.

In the case of a uniform rotor blade with a tip mass, where the rotor blade is composed of a flexible sheet or ribbon, the bifilar moment and propeller moment are caused by the radial stress and the mass distribution across the blade cross-section respectively. In this case, the propeller moment (nose-down) at any spanwise location is given by:

$$M_p(y) = I_\theta \Omega^2 \theta(R - y) + I_T \Omega^2 \theta_T \quad (10)$$

where x is the chordwise co-ordinate, y is the spanwise co-ordinate and θ_T is the angle of twist at the blade tip. The torsional moment of inertia of the blade (per unit length) is

$$I_\theta = \int_{chord} \rho t x^2 dx \quad (11)$$

The bifilar moment (nose-down) at any spanwise location is given by:

$$M_b(y) = \frac{\Omega^2(R^2 - y^2)}{2} I_\theta \theta' + I_T \Omega^2 R \theta_T' \quad (12)$$

Combining the above two moments, for uniform properties along the span, the equation of torsional motion of the blade is given by

$$-GJ\theta'' + I_\theta \ddot{\theta} + I_\theta \Omega^2 \theta - \frac{1}{2} I_\theta \Omega^2 [\theta'(R^2 - y^2)]' \quad (13)$$

with the boundary conditions

$$\theta(0) = 0 \quad (14)$$

$$GJ\theta'(R) = I_T(\ddot{\theta}_T + \Omega^2 \theta_T) \quad (15)$$

The solution of the above differential equation will yield the torsional frequencies of the system. A simple analysis of flutter and divergence boundaries can be performed considering a 2-D airfoil section undergoing vertical translational and pitching motion. The effective stiffness in the vertical translation and pitching degrees of freedom can be derived assuming a linear flap and torsion mode, as described by Winston.¹⁴ In

general, to achieve stable operation for any value of tip mass, the elastic axis should be ahead of the aerodynamic center, and the blade section center of gravity should be ahead of the elastic axis. Note that these results are valid for a rotor blade of low mass per unit length, with cables as the main structural members. In such a case, the elastic axis is determined by the position of the tip mass alone. However, in the present case of the flexible composite rotor where the tip mass is equal to the blade mass, the blade center of gravity is at mid-chord, and the location of the elastic axis does not depend only on the chordwise position of the tip mass. A more detailed analysis is required for the present case.

ANALYTICAL MODEL

The planform of the flexible rotor blades is shown in Figure. 4. The goal of the analytical study is to investigate the rotating frequencies and stability boundary of this rotor as a function of x_{CG} , the chordwise offset of the tip mass center of gravity from the mid-chord of the blade (forward is positive). In this study, the tip mass is approximately equal to the blade mass. The cross-section of a blade is shown in Figure. 5. Note that typically, $t \ll R$. The vertical position of the neutral axis is given by (with respect to the top surface of the blade cross-section)

$$y_1 = R \left[1 - \frac{2 \sin \alpha}{3\alpha} \left(1 - \frac{t}{R} + \frac{1}{2 - t/R} \right) \right] \quad (16)$$

The moments of inertia about the axes 1 – 1 and 2 – 2 are given by

$$I_1 = R^3 t \left[\left(1 - \frac{3t}{2R} + \frac{t^2}{R^2} - \frac{t^3}{4R^3} \right) \left(\alpha + \sin \alpha \cos \alpha - \frac{2 \sin^2 \alpha}{\alpha} \right) + \frac{t^2 \sin^2 \alpha}{3R^2 \alpha (2 - t/R)} \left(1 - \frac{t}{R} + \frac{t^2}{6R^2} \right) \right] \quad (17)$$

$$I_2 = R^3 t \left(1 - \frac{3t}{2R} + \frac{t^2}{R^2} - \frac{t^3}{4R^3} \right) (\alpha - \sin \alpha \cos \alpha) \quad (18)$$

The polar moment of inertia is given by $J = I_1 + I_2$. The Carbon fiber properties are assumed to be $E = 150$ GPa (along fiber) and $G = 0.0006$ GPa (across fiber). The later corresponds to shear modulus of a typical rubber like material. The density is $\rho = 3172.4$ kg/m³,

adjusted to generate the total measured mass of each blade. The sectional properties needed for a dynamic analysis follows from geometry and above material properties (see Table 1).

Property	Values
EA , N-m ²	8.453×10^5
EI_f , N-m ²	0.206
EI_t , N-m ²	41.920
GJ , N-m ²	1.685×10^{-4}
Mass per length, kg/m	0.0179

Table 1. Cross-sectional stiffness and mass properties of a carbon fiber blade.

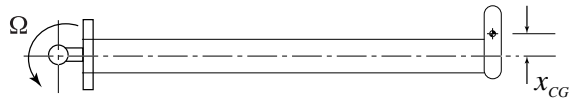


Figure 4. Schematic of rotor blade planform with tip mass

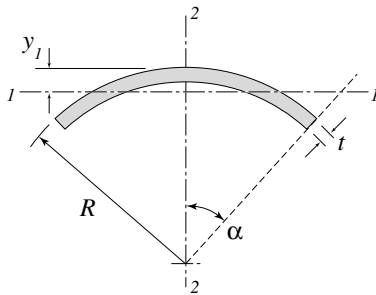


Figure 5. Rotor blade cross-section

The two-bladed hingeless rotor is modeled using non-linear beam finite elements within a well validated rotor comprehensive analysis UMARC²¹ (University of Maryland Advanced Rotorcraft Code). Both blades are assumed to be identical. Each blade is discretized into 20 finite elements undergoing flap, lag, torsion and axial degrees of motion. The rotor blades are modeled as second-order nonlinear, isotropic Euler-Bernoulli beams, extended to include axial elongation and elastic twist as quasi-coordinates. The resultant almost-exact beam model is accurate up to moderate bending deflections of 15% radius.

The flutter analysis uses the rotating frequencies calculated from the above finite element analysis to set up a classical rotary wing two degree of freedom pitch-flap model.²² A more detailed

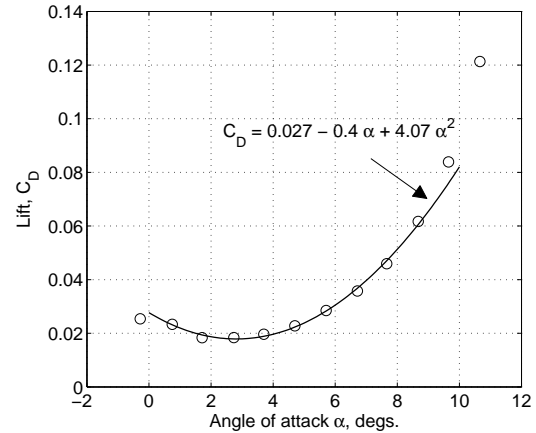


Figure 6. Circular arc airfoil drag coefficient: measurements and curve fit (Reference. 23)

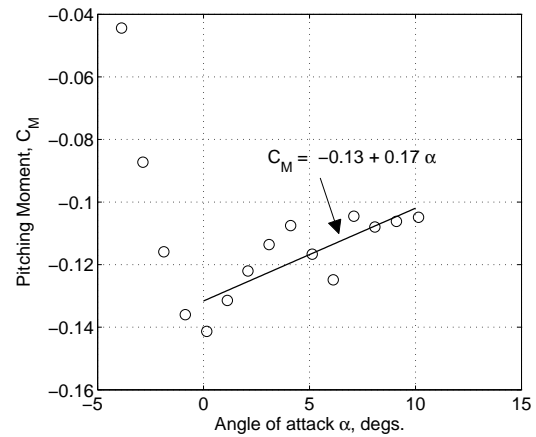


Figure 7. Circular arc airfoil 1/4-c pitching moment coefficient: measurements and curve fit (Reference. 23)

analysis is beyond the scope of this initial simple analysis. However, a 2-D Theodorsen unsteady aerodynamic model (thin airfoil, attached flow), is included. The sectional airfoil properties and the linear fits used in this study are shown in Figures. 6 and 7. These data were measured at a Reynold's number of approximately 300,000, and are reported in Reference 23. The drag and pitching moment test data are modified to reflect the Reynold's number of the present tests. The lift coefficient is represented as $C_l = 0.51 + 5.73 \alpha$, where $C_{l\alpha} = 5.73$ includes an aspect ratio correction. Additional drag due to the tip mass is neglected in the present analysis.

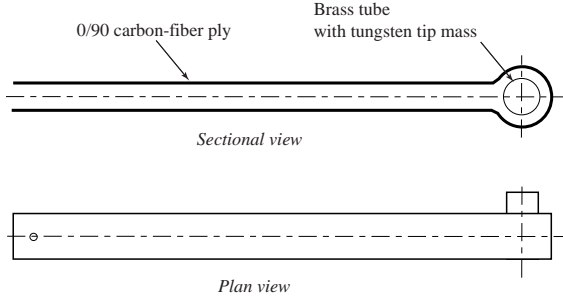


Figure 8. Schematic of flexible rotor blade fabrication

EXPERIMENTAL SETUP

The hover performance of two sets of untwisted, constant chord blades was measured by incorporating them in a two-bladed rotor system. The blades were fabricated in-house and had identical planforms as well as airfoil sections. One set of blades was rigid and the other set of blades was highly flexible.

Blade Fabrication

The rigid blades were fabricated using two plies of carbon-fiber cloth, oriented $\pm 45^\circ$ to the blade span. The plies were impregnated with a conventional room-temperature cure resin and were compressed in a mold. The resulting blades were stiff in torsion as well as in bending, and had the circular arc sectional profile imparted by the mold.

The flexible composite blades were fabricated using one ply of carbon-fiber cloth oriented along ($\pm 90^\circ$) the blade span. The ply was wrapped around a thin-walled brass tube at the tip end, as shown in Figure. 8, effectively forming a blade two plies thick. A tungsten rod of diameter 0.125 inches and length 0.75 inches could be inserted in the brass tube such that its chordwise position could be varied. The carbon-fiber plies were impregnated with a flexible polyurethane elastomer (Freeman 1035) and compressed in a mold. The resulting blades were extremely flexible but had the same sectional profile as the rigid blades. Note that the Young's modulus of the resulting composite is dominated by the carbon-fibers, while the shear modulus is dominated by the polyurethane elastomer.

The cross-section of the blades is as shown in Figure. 5, and the parameters of both the blades are given in Table. 2. A picture of one blade from each set is shown in Figure. 9.

	Rigid	Flexible
Rotor radius R_b , m	0.226	
Chord c , m	0.018	
Rotational speed, RPM	2100	
Thickness t , mm	0.65	
Section half-angle α , deg	13.15	
Camber, %	5.5	
t/c ratio, %	3.6	
Blade mass, g	3.78	4.89
Tip mass, g	-	4.65

Table 2. Rigid and flexible blade parameters

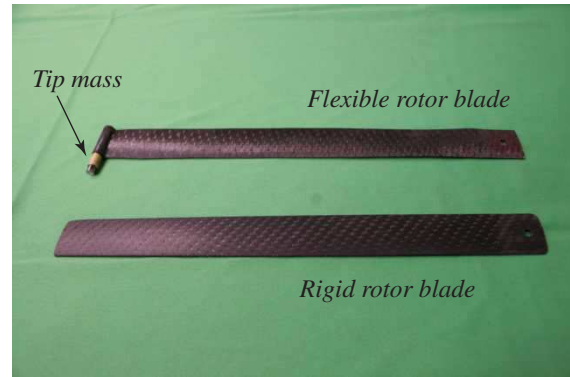


Figure 9. Rigid and flexible rotor blades on the hover test stand

Hover Test Stand

The performance of the blades in hover was measured on a test stand designed and built in-house. Figure. 10 shows a schematic of the hover test stand. The two-bladed rotor hub is mounted directly on a brushless outrunner DC motor. The motor (AXI 4130/20) was chosen to have a high torque and low speed constant so that it could directly drive a rotor of diameter up to 0.6 m, at a tip speed of up to 135 m/sec, without the need for a gearbox. The motor and rotor assembly was mounted directly on a six component strain gage load cell (ATI Mini40E), with a full scale rating of 5 lbs in the thrust direction. A magnetic pickup provided a 1/rev pulse, which was used to measure the rotational speed, as well as to perform synchronous averaging of all the signals. Data was acquired by a National Instruments CompactDAQ system with a custom virtual instrument programmed in Labview. The quantities measured were the rotor forces and moments in the fixed-frame, rotational speed, motor voltage and motor current. A picture of the flexible rotor blades mounted on the hover test stand is shown in Figure. 11.

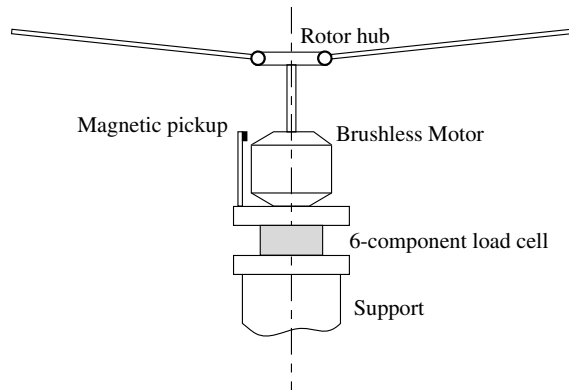


Figure 10. Hover test stand

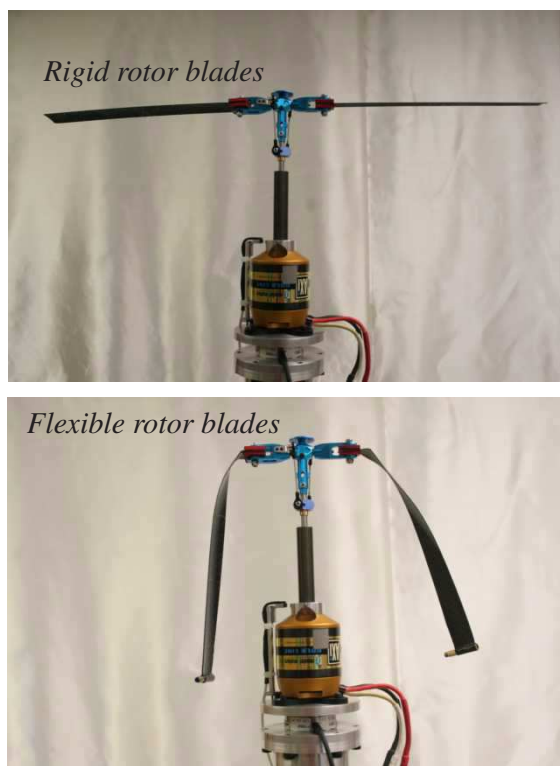


Figure 11. Rotor with flexible composite blades and tip mass mounted on the hover test stand

Test Matrix

The rigid and flexible blades were tested over a range of collective pitch angles from 0 deg to 21 deg. In the case of the rigid blades, the tests were stopped after measurements indicated that the blades were stalled. The testing was performed at a constant rotor speed of 2100 RPM. Based on the analysis, the chordwise position of the tip mass was adjusted so that the flexible blades were stable. At each collective pitch setting, data was collected over a period of ten

seconds. Synchronous averaging was performed with reference to the 1/rev trigger, and the resulting waveforms over one revolution were averaged to obtain a mean value of rotor thrust, rotor torque and rotational speed.

RESULTS AND DISCUSSION

Aeroelastic stability

The rotor frequencies calculated from the comprehensive analysis code are shown in Figure. 12 for a flexible composite rotor blade without any tip mass. The addition of tip mass changes the blade inertia in flap and torsion and therefore affects the frequencies. The frequency plots with the tip mass center of gravity located at the mid-chord is shown in Figure. 13. It can be seen that the addition of the tip mass brings the first torsion frequency closer to 1/rev and generates a second flap bending mode. The frequencies are all still uncoupled as there is no sectional offset - center of gravity, elastic axis, tension axis are all located at mid-chord. The aerodynamic center, however, is at 1/4-c. Therefore, the blade in this configuration is naturally unstable. The rotating frequencies of the flexible rotor blades are shown in Table.

The flutter and divergence boundaries are shown in Figure. 14. Due to the very low torsion frequency, there is a thin margin for locating the tip mass center of gravity. A location at the 1/4-c or within 2% behind the 1/4-c appears flutter free for this rotor. The blade becomes divergence free as the tip mass center of gravity is moved closer to 1/4-c. The analysis shows that it can be as far behind as 7.5%c from the aerodynamic center for a lower rotational speed.

At a higher rotational speed (2000 RPM) it must be moved up to at least 5.2%c behind the aerodynamic center to prevent divergence. However, flutter, not divergence, is the key design concern for this rotor. The stability margins remain nominally constant with RPM with a minor relief with increasing speed. Note that previous studies^{14, 18, 19} indicated that the stability margins were independent of rotor speed. The analysis also indicated that there exist regions of instability for tip mass center of gravity locations just ahead of 1/4-c, depending on the torsional frequency. Thus the design requires a careful study with both experiments and analysis.

The experiments were performed for several chordwise locations of tip mass to ascertain

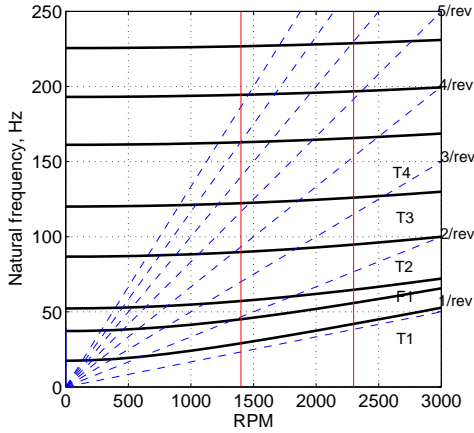


Figure 12. Frequency plot of flexible rotor blade without tip mass; blade mass 4 g

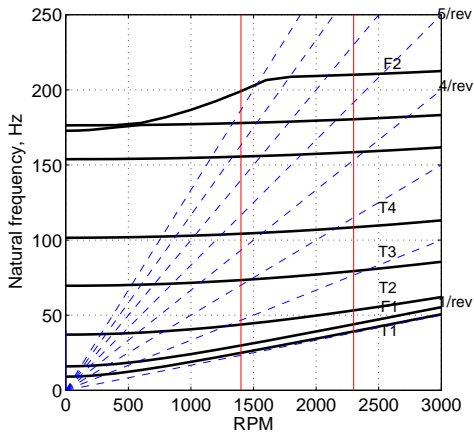


Figure 13. Frequency plot of flexible rotor blade with tip mass; blade mass 4 g, tip mass 4.5 g, centered at mid-chord

Rotational speed, RPM	ν_{β} , /rev	ν_{θ} , /rev
1300	1.308	1.079
2000	1.174	1.032
2400	1.139	1.021

Table 3. First flap and torsion frequencies of flexible rotor blade with tip mass centered at mid-chord

the stability boundary. The existence of instability was determined by observation of unsteady motion of the rotor tip path plane, a large increase in rotor noise, as well as an increase in rotor power. No data was collected in cases of unstable rotor operation. The data reported in this paper correspond to a tip mass positioned such that the

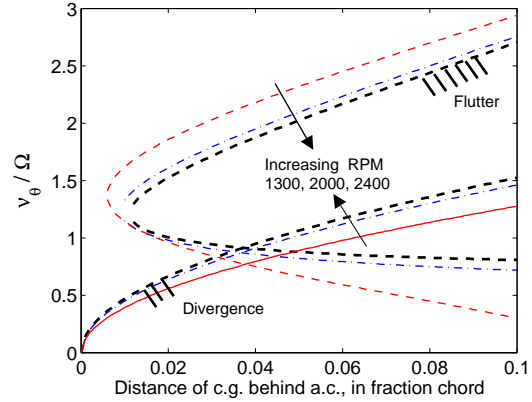


Figure 14. Pitch-Flap flutter and divergence boundaries for the carbon fiber rotor with respect to position of tip mass center of gravity; aerodynamic center (a.c.) at 1/4-c

center of gravity of the tip mass is close to the leading edge of the rotor blade. Based on the mass of the blade itself and the tip mass, this chordwise position corresponds to the center of gravity of the total blade (including tip mass) coinciding approximately with the aerodynamic center.

Measured rotor performance

The thrust produced as a function of collective pitch is shown in Figure. 15 for both the rigid as well as the flexible rotor blades. The trend for the rigid blades is as expected, showing a linear increase in thrust with collective pitch, and with a positive thrust at zero collective due to the cambered airfoil. In the case of the flexible blades, the thrust at zero collective is negative. This is attributed to the nose-down moment caused by gravity acting on the tip mass resulting in a net negative twist of the rotor blade. As the collective pitch of the flexible blades increases, the thrust produced increases approximately linearly, but is still significantly lower than the thrust produced by the rigid blades at the same collective. The large propeller moments on the tip mass tend to align the tip of the flexible blades close to flat pitch. Consequently, the flexible blades experience a large twist, especially at higher collective settings.

Figure. 16 shows the rotor Figure of Merit (FM) as a function of blade loading (C_T/σ) for both the rigid blades and the flexible blades. The maximum Figure of Merit achieved by the rigid

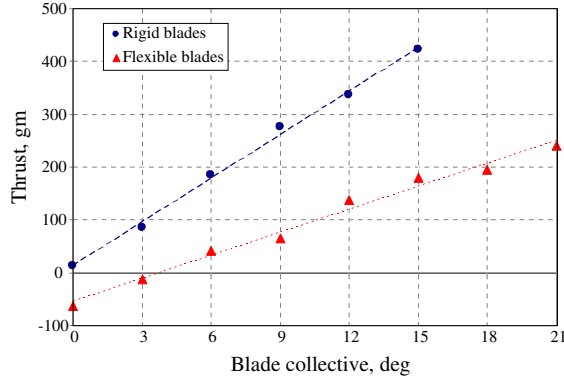


Figure 15. Comparison of thrust produced by rotors with rigid and flexible blades at 2100 RPM

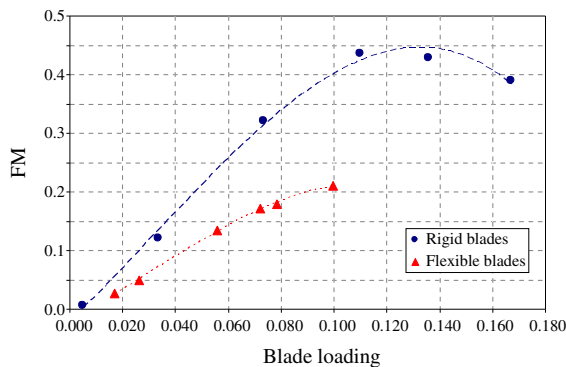


Figure 16. Comparison of Figure of Merit of rotors with rigid and flexible blades at 2100 RPM

blades is approximately 45%, which is consistent with previous studies on micro-helicopter rotor blades with rectangular tips and blunt leading edges.^{12,13,20} This maximum value can be significantly increased by sharpening the leading edge of the blades as well as incorporating a specific tip shape. The maximum Figure of Merit of the flexible blades is around 22%, however it can be seen that the rotor is not stalled even at the relatively high collective pitch of 21 deg. The low Figure of Merit compared to the rigid rotor blades can be attributed to the large drag caused by the tip mass, as well as portions of the blade at large angles of attack. As the stability of the blade and a baseline performance with a tip mass has been established, careful design of a low drag tip mass distribution can improve the flexible rotor performance. In addition, the possibility of extending the rotor radius to achieve a lower disk loading rotor is expected to mitigate the poor efficiency of the flexible rotor blades.

SUMMARY AND PLANNED ACTIVITIES

A rotor with extremely flexible composite rotor blades was fabricated and tested in hover. The flexibility of the blades was such that they could be rolled up and stowed in the rotor hub. The design of the rotor blades was focused toward application on a micro-helicopter. Accordingly, the blades had a circular arc airfoil section with 5.5% camber, untwisted, constant chord planform, and a span consistent with a rotor diameter of 18 inches. A tip mass equal to the mass of the blade was used to stabilize the flexible rotor. A comprehensive rotorcraft aeromechanics code was used to analyze the behavior of the flexible rotor blades in hover and to calculate the effect of the tip mass on rotor stability. The hover performance of a two-bladed rotor with the flexible blades was compared to that of a rotor with rigid blades having identical planform and airfoil profile.

The analysis indicated stable rotor operation for chordwise positions of the tip mass center of gravity within a range 10% of the chord aft to slightly forward of the aerodynamic center of the blade. The stability boundary was found to have a minor dependence on the rotor speed, with a larger allowable tip mass center of gravity range at higher rotational speeds.

The flexible blades exhibited stable operation in hover with a tip mass center of gravity located approximately at the blade leading edge. Measurements of the hover performance indicated a maximum Figure of Merit of 44% for the rigid rotor blades and 22% for the flexible rotor blades. In addition, due to a large induced twist, the flexible rotor blades produced lower thrust compared to the rigid blades. However, blade stall was not observed in the flexible rotor blades even at a relatively high collective pitch of 21 degrees. The poor efficiency of the flexible blades is attributed to a combination of an unfavorable twist distribution as well as large drag of the tip mass. It can be concluded that the concept of an extremely flexible composite rotor blade is feasible, however careful design is required to achieve an efficiency comparable to a rotor with rigid blades of the same diameter.

Future plans involve systematic testing of the flexible rotor blades with a fairing around the tip mass, as well as a redistribution of mass to improve the rotor efficiency. Bending-torsion

coupling will be investigated to enable stable rotor operation without any need for tip mass. Finally, the analysis as well as experimental program will be extended to investigate the behavior of the rotor in forward flight.

References

- [1] Fradenburgh, E. A., "The High Speed Challenge for Rotary Wing Aircraft," *SAE Paper #911974, Proceedings of the 29th International Pacific Air & Space Technology Conference, Nagoya City, Japan*, October 1991, pp. 91-109.
- [2] Ludi, L. H., "Composite Aircraft Design," *Journal of the American Helicopter Society*, Vol. 13, No. 1, January 1968, pp. 1-10.
- [3] Linden, A. W., "Fifty Years of Sikorsky High Speed Concepts," *American Helicopter Society 64th Annual Forum Proceedings, Montreal, Canada*, April 29 - May 1 2008.
- [4] Cheney, M. C. J., "The ABC Helicopter," *Journal of the American Helicopter Society*, Vol. 14, No. 4, October 1969, pp. 10-19.
- [5] Burgess, R., "The ABC Helicopter - A Historical Perspective," *American Helicopter Society 60th Annual Forum Proceedings, Baltimore, MD*, June 7-10 2004.
- [6] Blackwell, R., and Millott, T., "Dynamics Design Characteristics of the Sikorsky X2 Technology Demonstrator™ Aircraft," *American Helicopter Society 64th Annual Forum Proceedings, Montreal, Canada*, April 29 - May 1 2008.
- [7] Bagai, A., "Aerodynamic Design of the X2 Technology Demonstrator™ Main Rotor Blade," *American Helicopter Society 64th Annual Forum Proceedings, Montreal, Canada*, April 29 - May 1 2008.
- [8] Mitchell, C., and Vogel, B., "The Canard Rotor Wing (CRW) Aircraft - A New Way to Fly," *AIAA Paper# AIAA-2003-2517, Proceedings of the AIAA International Air and Space Symposium and Exposition: The Next 100 Years, Dayton, Ohio*, 14-17 July 2003.
- [9] Ryan, T. C., and Girard, P. F., "Flexible Blade Retractable Rotor Aircraft," January 1972 US Patent 3,637,168.
- [10] Feldman, L., "Flexible Sail Rotor Devices," January 1972 US Patent 3,633,850.
- [11] Fuller, B. L., "Rollable Airfoil," December 1984 US Patent 4,485,991.
- [12] Pines, D. J., and Bohorquez, F., "Challenges Facing Future Micro-Air Vehicle Development," *Journal of Aircraft*, Vol. 43, No. 2, April 2006, pp. 290-305.
- [13] Chopra, I., "Hovering Micro Air Vehicles: Challenges and Opportunities," *Proceedings of International Forum on Rotorcraft Multidisciplinary Technology, Seoul, Korea*, October 2007.
- [14] Winston, M. M., "An Investigation of Extremely Flexible Lifting Rotors," Langley Research Center, National Aeronautics and Space Administration NASA TN D-4465, Langley Station, VA, April 1968.
- [15] Winston, M. M., "A Hovering Investigation of An Extremely Flexible Lifting Rotor," Langley Research Center, National Aeronautics and Space Administration NASA TN D-4820, Langley Station, VA, October 1968.
- [16] Pruyn, R. R., and Swales, T. G., "Development of Rotor Blades with Extreme Chordwise and Spanwise Flexibility," *American Helicopter Society 20th Annual National Forum Proceedings, Washington D. C.*, 13-15 May 1964, pp. 102-108.
- [17] Katzenberger, E. F., and Carter, E. S., *Vertical Flight: The Age of the Helicopter* Smithsonian Institution Press, for the National Air and Space Museum, Washington D. C., 1984, Ch. The Technical Evolution of Sikorsky Helicopters, 1950-83, pp. 193-219.
- [18] Goldman, R. L., "Some Observations on the Dynamic Behavior of Extremely Flexible Rotor Blades," *IAS Paper No. 60-44, Presented at the 28th Annual Meeting of the IAS, New York, Jan. 25-27*, 1960.
- [19] Roeseler, W. G., "The Effect of Ribbon Rotor Geometry on Blade Response and Stability," Master's thesis, Massachusetts Institute of Technology, May 1966.
- [20] Hein, B., and Chopra, I., "Hover Performance of a Micro Air Vehicle: Rotor at Low Reynolds Number," *Journal of the American Helicopter Society*, Vol. 52, No. 3, July 2007, pp. 254-262.
- [21] Datta, A., and Chopra, I., "Validation and Understanding of UH-60A Vibratory Loads in Steady Level Flight," *Journal of the American Helicopter Society*, Vol. 49, No. 3, July 2004, pp. 271-286.
- [22] Johnson, W., *Helicopter Theory* Dover Publications Inc., New York, NY, 1994.
- [23] Wallis, R. A., "Wind Tunnel Tests on a Series of Circular Arc Airfoils," *ARL Aero Note 74*, 1946.